Energy efficient control of polychromatic solid-state lighting using a sensor network

Matthew Aldrich[a], Nan Zhao[b], and Joseph Paradiso[a]

[a]MIT Media Lab, Responsive Environments Group, Cambridge, MA 02139, USA;
[b]RWTH Aachen University, MedIT, D-52074 Aachen, Germany

ABSTRACT

Motivated by opportunities in smart lighting, energy efficiency, and ubiquitous sensing, we present the design of polychromatic solid-state lighting controlled using a sensor network. We developed both a spectrally tunable light source and an interactive lighting testbed to study the effects of systems that adjust in response to changing environmental lighting conditions and users' requirements of color and intensity. Using both linear and nonlinear optimization, the setpoints of overdetermined systems (greater than three wavelengths) and the energy consumption of the network are adjusted according to the room's lighting conditions (e.g., lux and color temperature of multiple fixtures). Using these techniques, it is possible to maximize luminous efficacy or the color rendering index for a given intensity and color temperature. We detail the system modeling, design, optical calibration, and control theory required to modulate the luminous output and minimize wasted energy.

Keywords: Solid state lighting, energy efficiency, sensor networks, optimization, spectral control, color rendering, LEDs

1. INTRODUCTION

Occupants of near-future buildings will not necessarily be able to flip a light switch or adjust a thermostat to control building utilities. There may well be too many devices to easily control with direct "switches," and instead they will need to be driven by inferred intention or simple, intuitive, collective control. More crucially, as about 40% of the energy used in the US and most developed economies tends to be consumed in homes and buildings,[1] energy conservation concerns will pull our hand off the dial as environments will regulate themselves in order to accommodate occupants' objectives and best tend to their comfort while minimizing energy consumption. Accordingly, smart energy management will be a needed and motivating application area of solid-state lighting, as user state, behavior and context are measured, inferred, and leveraged across a variety of domains and environments using sensors and actuators to mitigate energy usage.

Lighting, in particular, accounts for 22% of all electricity consumed in the United States.[2] While simple motion sensors are now commonly integrated into new buildings to turn lights off when occupants leave an illumined area, they provide very coarse control input, often causing more area than is necessary to be lit or mistakenly turning lights off when an occupant stays still for too long. As we move into robustly sensed and finely actuated environments, lighting will become richly responsive, dynamically adapting to users' needs while mitigating energy use.

In this research, we attempt to minimize the energy spent lighting while simultaneously maximizing utility and the photometric characteristics of the light source. In the past, optimal control of lighting networks has been researched using traditional lighting such as incandescent and fluorescent technologies.[3,4] Lighting networks comprised of active emitters present the greatest challenges of control, as strictly linear techniques guarantee an exact solution for chromaticity but often with a low color rendering index (CRI). If the control of an active emitter or hybrid active/phosphor system is reformulated as an optimization, then the setpoints for a given color

Further author information: (Send correspondence to M.A.)
M.A.: E-mail: maldrich@media.mit.edu
N.Z.: E-mail: nan.zhao@rwth-aachen.de
J.P.: E-mail: joep@media.mit.edu

temperature can be found within the limits of a four-step MacAdam ellipse, or at maximum distance from the blackbody curve. Using these techniques, we construct several devices using commercially available LEDs and demonstrate the effectiveness of these methods.[5]

Achieving these goals requires solving two problems. The first problem, handled offline, is the global optimization solved using gradient-free techniques to find the setpoints for a five wavelength LED array for multiple color temperatures. The second problem, which is continuously solved in realtime, is the minimization of the lighting network's power consumption using feedback from the user and environment. In this local optimization problem, the illuminance and color at a point of interest (i.e., where the sensor node is placed) is set by the user. The amount of ambient light and the contribution of each light source in the network are measured (Figure 1). The intensity of each fixture is solved by a linear program. The activity vectors correspond to the illuminance measured at the incident surface and the decision variables correspond to the forward current of the light sources. The objective function penalizes the net lighting current to minimize net energy. In lighting networks comprised of white LEDs, the optimal control of the network simplifies to a linear program, as reducing the current will not cause chromaticity shift. To test this specific implementation, we created an interactive lighting testbed comprised of color tunable phosphor-based luminaires.[6]

Although the desired illuminance is satisfactorily represented as a linear constraint, the greatest challenge to building intelligent networks using LEDs is emitter variance, temperature dependence, and the difficulties of controlling a network comprised of a large number of variables (i.e., the number of wavelengths to be controlled). The control problem is further complicated by issues of optical sensor variance, occlusion of the sensor, and network update rates (e.g., estimating dark lighting levels, polling sensor nodes, and preprocessing the data). To the user, minimal control is required, as the lighting network must be capable of energy efficient operation without the direct intervention and constant adjustment by the user. In previous research, the use of commercially available sensor nodes imposed limited flexibility and control of these systems. Fixed resolution and no guarantees of timing or update rates were among the greatest problems faced by researchers who favored a top down approach.

This work extends previous research regarding sensor-enabled light control, in that solid-state lighting is considered to be the primary means of illumination. Consequently, the lighting network can optimize the light output for greater efficiency or higher color quality depending on the measured ambient conditions. Whereas previous research considered one linear parameter, illuminance, we extend the control methods to highly nonlinear photometric and color criteria that directly govern energy consumption and visual quality. We also incorporate a low-cost color sensor to use color temperature as a feedback parameter and describe the performance of this method. Additionally, we present the energy savings of lighting networks comprised of both active and phosphor-converted LEDs.

2. RELATED WORK

Dynamic and adaptive lighting enabled by environmental sensors offers additional energy savings. Early work by Crisp and Hunt in the 1970s focused on estimating internal illuminance from artificial and external light sources in order to reduce unnecessary lighting and excess energy expenditure.[7–11] This early work discussed the use of photosensors to monitor the natural daylight in the office place. With the availability of low cost lux sensors (perhaps more importantly, silicon improvements to reign in device variance) and an influx of low cost embedded devices, this simple form of intensity feedback was extended to networks of fixed color incandescent and fluorescent lights. More recently (2005), Singhvi et al. designed and tested closed loop algorithms to maximize energy efficiency while meeting user lighting requirements in an incandescent lighting network.[3] Park et al. developed a lighting system to create high quality stage lighting to satisfy user profiles.[12] Wen et al. researched fuzzy decision making and Bayesian inference in lighting control networks.[4] Machado and Mendes tested automatic light control using neural networks, as did Mozer in a pioneering study from 1992, where light switches and thermostats in his house provided reinforcement for a neural network that incorporated motion sensors to build a user activity model to automatically control utilities.[13,14]

As early as 2002, Muthu et al. incorporated optical and temperature feedback into the LED driver architecture, allowing for compensation of optical, electrical and thermal variations of the system.[15] Subsequent research

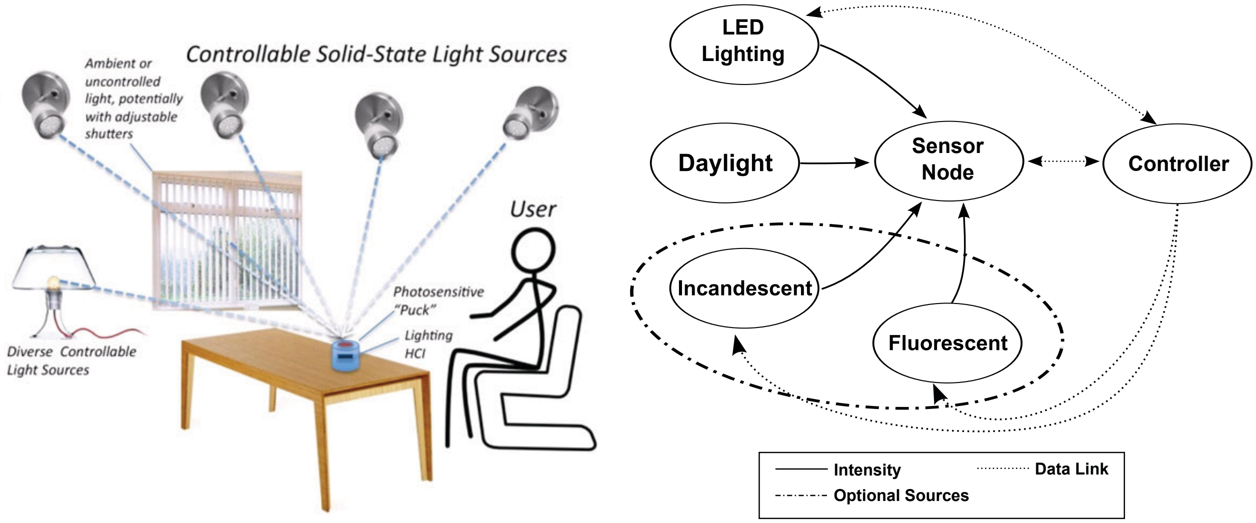

(a) (b)

Figure 1: In (a), a high level diagram of the interactive control environment. In (b), the lighting network consists of LED light sources, optional incandescent and fluorescent sources, and ambient room conditions (daylight), that are measured by a single or group of sensor nodes. The sensor nodes return intensity and color information back to the control node (e.g., a computer) for processing. Here, the intensity is controlled via a link to the artificial light sources. The data link is bidirectional from either the sensor node or the LEDs.

evaluated the use of neural networks to maintain accurate chromaticity[16] and explored optical feedback using three or more unique LED wavelengths.[15,17] This is achieved by fixing the ratio of intensity at one wavelength to another at the cost of saturated colors and a decreased color gamut. This does not guarantee the best color rendering index for a given white point. The optimal method to create white light using LEDs is still an open question, and while several strategies exist, there are tradeoffs between efficacy and color rendering ability.[18]

Common approaches using active emitters include dichromatic (blue and yellow), trichomatic (red, green, blue), and tetrachromatic (red, green, blue and cyan or yellow) sources.[19–24] In these papers, the authors report on the effects of dominant wavelength, correlated color temperature (CCT), and resulting color rendering index. Lei et al., uses a simplistic technique in the evaluation of four wavelengths and Zukauskas et al. applies an exhaustive boundary search to maximize certain optical properties of polychromatic light sources, yet does not provide any information on completion time or provide any empirical results of the study.[20] Ultimately, in each of the papers, the authors provide the theoretical “best” combination of wavelengths and intensities to maximize either the ratio of flux to radiant energy, or to maximize the color rendering index for a given color temperature.

The problem is that these techniques do not correspond with the ranges of dominant wavelengths provided by the manufactures, nor do they take into account the variance in intensity and dominant wavelength across a particular bin of LEDs. In essence, the conclusions of these papers restrict the applicability of the results to either highly specialized configurations or particular laboratory and operating environments. While performing a sensitivity analysis is one way to at least understand these effects, a better approach is to remain flexible from the start – specifically, to concentrate on adaptive techniques that require no assumptions of the system. By taking into account the variance of the LEDs and other uncontrollable parameters upfront (i.e., creating a model based on the measured irradiance of the system), we free ourselves from heuristic based assumptions about the wavelengths and required intensity of the LEDs.

3. SPECTRAL OPTIMIZATION USING LINEAR AND NONLINEAR METHODS

Traditional methods of color control assume a linear relationship between the setpoint and the output. In these problems, the exact solution is found by solving the linear equality $\mathbf{Ax} = \mathbf{b}$ for $\mathbf{x}$. However, the system could also be formulated with more equations than unknowns, hence $\mathbf{x}$ is overdetermined and no exact solution exists. In this case, a common technique uses the pseudoinverse to minimize the sum-squared error between $\mathbf{Ax}$ and $\mathbf{b}$, resulting in an exact minimum square error solution if $\mathbf{A}$ is non-singular. While these approaches work well to calibrate most optical sensors (e.g., those in scanners, cameras, etc.), they are not necessarily optimal for lighting. In this section, we introduce several nonlinear techniques which optimize the color rendering index for an arbitrary color.

3.1 Exact and Minimum Square Error Solutions

We are interested in the relationship between a setpoint and the resulting color. If the lighting system is comprised of three wavelengths, (e.g., red, green, and blue) then the relationship is of the form $\mathbf{Ax} = \mathbf{b}$, where matrix $\mathbf{A}$ is the measured tristimulus values, $\mathbf{x}$ is the setpoint, and $\mathbf{b}$ is the tristimulus value of the resulting setpoint. Solving this equation for $\mathbf{b}$ allows us to specify the white point :

$$\begin{pmatrix} X_r R_{set} & X_g G_{set} & X_b B_{set} \\ Y_r R_{set} & Y_g G_{set} & Y_b B_{set} \\ Z_r R_{set} & Z_g G_{set} & Z_b B_{set} \end{pmatrix}^{-1} \begin{pmatrix} X \\ Y \\ Z \end{pmatrix} = \begin{pmatrix} R \\ G \\ B \end{pmatrix}. \tag{1}$$

If we add a fourth wavelength to the system, a simple approach is to fix the ratio of this fourth wavelength to its closest color.[17] For example, if we add an amber color, we make amber a fixed ratio, α, of the red setpoint. In this example, the solution is

$$\begin{pmatrix} X_r(\lambda_1) + X_r(\lambda_2) & X_g & X_b \\ Y_r(\lambda_1) + Y_r(\lambda_2) & Y_g & Y_b \\ Z_r(\lambda_1) + Z_r(\lambda_2) & Z_g & Z_b \end{pmatrix}^{-1} \begin{pmatrix} X \\ Y \\ Z \end{pmatrix} = \begin{pmatrix} R \\ G \\ B \end{pmatrix}, \tag{2}$$

where

$$\begin{pmatrix} R \\ A \\ G \\ B \end{pmatrix} = \begin{pmatrix} R \\ \alpha R \\ G \\ B \end{pmatrix}. \tag{3}$$

If we consider a linear system of the form $\mathbf{Ax} = \mathbf{b}$ that contains five wavelengths, then we can rewrite matrix $\mathbf{A}$ as a 3-by-5 system. However, $\mathbf{A}$ is now rectangular and has more equations than unknowns, $\mathbf{x}$ is overdetermined, and, no exact solution exists. But, we could seek a solution of $\mathbf{x}$ that minimizes the sum-squared error between $\mathbf{Ax}$ and $\mathbf{b}$, such as $J_s(\mathbf{x}) = \|\mathbf{Ax} - \mathbf{b}\|^2$. In this classical problem, the norm has a closed form solution, and we solve for the Jacobian by taking the derivative of $J_s(\mathbf{x})$ and setting the solution equal to zero. Solving this leads to the pseudoinverse:

$$\begin{aligned} \mathbf{x} &= (\mathbf{AA})^{-1}\mathbf{A}^T\mathbf{b} \\ &= \mathbf{A}^\dagger\mathbf{b}. \end{aligned} \tag{4}$$

Using the five wavelength example to illustrate a red, amber, green, cyan, and blue system:

$$\begin{pmatrix} R \\ A \\ G \\ C \\ B \end{pmatrix} = \begin{pmatrix} X_r & X_a & X_g & X_c & X_b \\ Y_r & Y_a & Y_g & Y_c & Y_b \\ Z_r & Z_a & Z_g & Z_c & Z_b \end{pmatrix}^\dagger \begin{pmatrix} X \\ Y \\ Z \end{pmatrix}, \tag{5}$$

where the 3-by-5 tristimulus matrix is measured with some illuminance and the subscripts denote the measured wavelength such that solution $\mathbf{x}$ is of the set $\{\mathbf{x} \in \mathbb{R}^n : 0 \leq \mathbf{x} \leq 1\}$ where the dimension of the space is n, the number of wavelengths. Using this method, we are guaranteed that for any color temperature, a minimum square error solution exists. Therefore, in contrast to the method in Equation (2), we are no longer tasked with finding the ratio α such that we minimize error for any color temperature.

3.2 Linear Calibration of a Color Sensor to Measure Color Temperature

A color sensor can be added to measure the correlated color temperature of incident light or to control and maintain accurate chromaticity. In this paper, we describe the use of a three channel (red, green, and blue) color sensor to measure the CCT of incident light. We calibrate the sensor with n samples such that:

$$\begin{pmatrix} X \\ Y \\ Z \end{pmatrix} = \left(\mathbf{TS}^{\dagger}\right) \begin{pmatrix} R_s \\ G_s \\ B_s \end{pmatrix}. \tag{6}$$

The matrix $\mathbf{T}$ is of size 3-by-n and contains the X, Y, and Z tristimulus values as measured by a spectrometer or colorimeter. $\mathbf{S}$ is a 3-by-n matrix containing the respective color sensor readings that correspond to each column entry in the tristimulus matrix such that $n \geq 3$. Using these tristimulus values, the color temperature is calculated according to Robertson's method.[25] These two matrices are created during the sensor calibration step. Subsequent calculations use this transfer function and the current sensor reading to calculate the tristimulus values.

Additional details on chromaticity feedback and control are given in Ref. 5.

3.3 Optimizing the Power and Color Rendering of a Lighting Network

Direct search methods are a class of optimization algorithms that require only a numerical answer, supplied by the iterative evaluation of the objective, that guides the search. In general, these methods are applicable to problems that lack a closed form solution, or are non-convex, or discontinuous. In this research, the mesh adaptive direct search algorithm (MADS)[26] and generalized pattern search[27] are used to solve the global optimization problem. The algorithms are implemented in MATLAB as part of the Global Optimization Toolbox.[28] These techniques are similar to the classical methods of Jones et al.,[29] Hooke and Jeeves,[30] Rosenbrock,[31] and the Simplex algorithm.[32]

Consider n artificial light sources, where each light source consists of m wavelengths, where the ith wavelength is designated λ_i, the jth light source designated L_j and i and j are indexing variables of the set $\{i \in \mathbb{Z} : 1 \leq i \leq m\}$ and $\{j \in \mathbb{Z} : 1 \leq j \leq n\}$. If we consider the light source as a spherical point source, then for every λ_i in L_j there is a maximum illuminance, E_{ij}, incident on a plane at some distance d from the point source. In the presumed linear system, the intensity of any single wavelength λ_i in light source L_j with corresponding maximum intensity $\hat{I}_{v,ij}$, a forward current denoted I_p, a corresponding point on the blackbody curve (T_c), and a corresponding color rendering index ($\mathrm{R_a}$), is set by x where $\{x \in \mathbb{R}^{mn} : 0 \leq x \leq 1\}$.

The optimal setpoint x has the form: $\min_{x\in\Omega} f(x)$ where $f : \Omega \subset \mathbb{R}^{mn} \to \cup\{\infty\}$ and Ω is a set of feasible points subject to linear or nonlinear constraints. The function f does not have a closed form and is non-differentiable. Because there is no direct form of f, an optimization algorithm is required that is driven according to the results of f. We define f to be a scaled objective function to minimize square error with z representing our minimization goal:

$$\min_{x\in\Omega} f(x) = \begin{cases} \left(\frac{\hat{T}_c - T_c(x)}{\hat{T}_c}\right)^2 + \Delta uv(T_c)^2 + \left(\frac{\sum_{j=1}^{n} V_{in,j} \sum_{i=1}^{m} x_{ij} I_{p,ij}}{\sum_{j=1}^{n} V_{in,j} \sum_{i=1}^{m} I_{p,ij}}\right)^2 & \text{for } z = 0 \\ \left(\frac{\hat{T}_c - T_c(x)}{\hat{T}_c}\right)^2 + \Delta uv(T_c)^2 - \left(\frac{\mathrm{R_a}(x)}{100}\right)^2 & \text{for } z \neq 0 \end{cases} \tag{7}$$

subject to linear inequality constraints

$$\sum_{j=1}^{n}\sum_{i=1}^{m} k_j x_{ij} \hat{I}_{v,ij} \geq E_{desired} - E_{dark}, \tag{8}$$

$$\sum_{j=1}^{n}\sum_{i=1}^{m} k_j x_{ij} \hat{I}_{v,ij} \leq E_{desired} - E_{dark} + \beta(E_{desired} - E_{dark}), \tag{9}$$

where

$$k_j = \frac{E_{v,j} - E_{dark}}{I_{v,j}}. \tag{10}$$

The optimization problem is defined as a piecewise objective function whose goal is either minimizing energy (i.e., maximize efficacy) or maximizing the color rendering index for a specified color temperature, $\hat{T}_c$. The parameter $\Delta uv(T_c)$ is an error measurement of T_c designed to ensure that the white point defined by the feasible points is a high quality one. The left hand side of Equation (8) and Equation (9) can be replaced with the illuminance data directly measured by the sensor node and appropriately weighted by its contribution relative to the total measured lux (the k_j term). The term $E_{desired}$ describes the total lux required at the point of measurement. The dual inequality constraints (rather than a single linear equality constraint) are required to reduce the sensitivity to noise, and to allow the objective function f some flexibility as T_c, $\mathrm{R_a}$, and $E_{desired}$ can not be completely decoupled from each other (Principal Component Analysis could be used to show the extent of which these terms are linearly separable). The functions to calculate T_c, $\Delta uv(T_c)$, and $\mathrm{R_a}$ comprise the evaluation function of the algorithm.

If phosphor-converters are used, then the single goal is to minimize the power consumed by the network and is achieved using a linear program such that:

$$\min_x f(x) = \sum_{j=1}^{n} V_{in,j} \sum_{i=1}^{m} x_{ij} I_{p,ij} \text{ s.t.} \begin{cases} \sum_{j=1}^{n}\sum_{i=1}^{m} k_j x_{ij} \hat{I}_{v,ij} = E_{desired} - E_{dark} \\ 0 \leq x_{ij} \leq 1, \{x \in \mathbb{R} : 0 \leq x \leq 1\} \end{cases}, \tag{11}$$

where k_j is the same as Equation (10).

4. IMPLEMENTATION

The typical system is comprised of a sensor node, daylight, and incandescent, fluorescent, and LED technologies (see Figure 1b). Daylight, incandescent, and fluorescent sources are measured but uncontrolled in the present implementation. If the non-solid-state light sources can be modulated or switched, they can be included in our control scheme as well. The sensor node measures the intensity and color temperature of all sources and sends the data to a controller (in this research, a computer). The controller processes the data and, taking into account the user's preferences, sets the lighting to the optimal conditions. This method can be extended for multiple control nodes.

We designed a prototype LED lighting system and sensor board. The intensity of the LED fixture is controlled using 16-bit pulse width modulation (PWM). This requirement is crucial, since much of the theory requires that the power and intensity relationship of the light fixture be linear. A digital signal processor (DSP) with microcontroller-type peripherals controls the intensity, monitors on-board LED operating temperature, intensity and color, and has a bidirectional data link to the computer. The sensor node measures intensity and color. These data allow the controller to estimate the illuminance and correlated color temperature of each light source. The sensor node also features basic controls for the user (e.g., intensity and color control), and detects occupancy. Table 1 lists the parameters associated with the sensor node. The LED array used in this research consists of five unique wavelengths, four of which are active emitters and one that is phosphor-converted (Table 2). The five colors employed are royal blue, cyan, green, phosphor-converted amber, and red. Selecting a phosphor-converted amber allows for a higher efficiency and less temperature dependence. The LED array also has on-board temperature

Table 1: Illuminance sensor table for the sensor node. The sampling frequency of the analog sensors is 30 kHz. The sampling frequency (integration time) of the digital sensor is controlled by the sensor node. It is nominally set to 120 Hz, with variable oversampling set at 2×(up to 10×).

Sensor	Type	Bandwidth	Range	ADC Res.	mlx / mV
ISL29006, Intersil	analog, linear	50 Hz	2000 lux	2^{12}	606 mlx/mV
ISL29006, Intersil	analog, linear	600 Hz	2000 lux	2^{12}	606 mlx/mV
ISL29006, Intersil	analog, linear	50 Hz	10000 lux	2^{12}	3030 mlx/mV
TCS3414CS, Taos	digital, linear	50 Hz	5000 lux	2^{16}	1515 mlx/mV

Table 2: Description of the color, dominant wavelength, full width half maximum, efficacy and full part number of the LEDs used to test the system.

Color	Dominant Wavelength	FWHM	lm / W	Lumiled Part
Royal Blue	440nm - 460nm	30 nm	350 mW/W	LXML-PR01-0350
Cyan	490nm - 520nm	30 nm	70 lm/W	LXML-PE01-0070
Green	520nm - 550nm	24 nm	70 lm/W	LXML-PM01-0070
Amber (Phosphor)	587.8nm - 595.4nm	80 nm	70 lm/W	LXM2-PL01-0000
Red	620.5nm - 645nm	20 nm	40 lm/W	LXML-PD01-0040

sensors (to estimate LED junction temperature) and can measure, using filters, the red, green, blue, and clear values of the irradiance using a TCS3414 color sensor.

To test the control and feedback of the linear phosphor-based system, we created a testbed using four commercially available whitepoint adjustable luminaires (Figure 7).

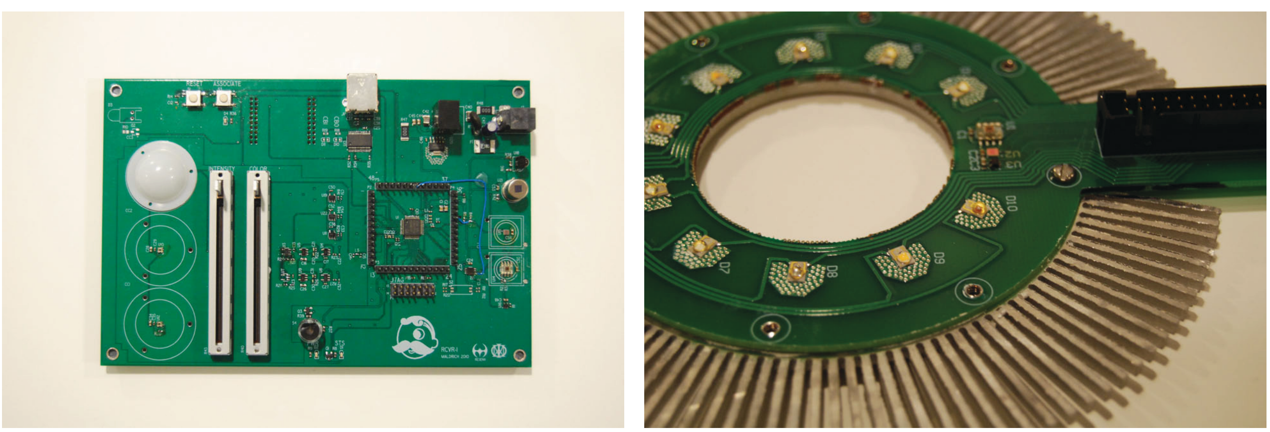

(a) (b)

Figure 2: The prototype sensing and control hardware (left) and LED array (right) used in the experiments to evaluate the nonlinear optimization of multiple photometric properties and dynamic control of illuminance. The sensor node was also used in subsequent experiments with the phosphor-based system.

5. RESULTS

5.1 Optimization and Calibration

To prepare the system for closed-loop operation, the individual spectra were collected for a single fixture using a spectrometer. It was assumed (at the expense of chromaticity error), that subsequent systems of the same LEDs and forward currents would use this single model. During this procedure, the power consumption of the test fixture was also measured using a digital multimeter. Figure 3b shows the measured irradiance of the system, as well as the superposition of the individual LEDs. The difference in the peaks between the two datasets is due to increased junction temperature during whitepoint measurement. Correcting this difference allows for improved setpoint accuracy across a greater range of color temperatures and intensities. Therefore, after acquiring the spectra, we apply a correction factor to the individual LED measurements according to:

$$\min_{\mathbf{x}} f(\mathbf{x}) = \sum_{j=1}^{n} \|E_{e,wp}(\lambda) - \sum_{i=1}^{m} \mathbf{x}_i E_{e,i}(\lambda)\|^2, \tag{12}$$

subject to $\{\mathbf{x} \in \mathbb{R} : 0 \leq \mathbf{x} \leq 1\}$. In this case, m is the total wavelengths in the measured system and n is the total number of white points taken, for example, with increasing intensity. Equation (12) seeks to find a correction factor for each wavelength present in the system such that the sum-squared error is minimized over multiple white points (e.g., multiple operating temperatures). The corrected spectra for each wavelength measured at the maximum PWM setting was used to build the model of the system. The calculation of the illuminance, color temperature, and color rendering index of the setpoints was performed in MATLAB according to the formulae provided by Wyszecki and Stiles.[33]

Using these models of spectral output and power consumption, we first performed a Monte Carlo simulation for a fixed illuminance at 30 cm to visualize the possible solutions (Figure 3a). Next, we generated several test sets of data for 11 different color temperatures (2800 K – 10000 K) at three different illuminance levels (500 lx, 1000 lx, and 1500 lx at 30 cm) and measured the resulting photometric and electrical data (Figure 4). Subjectively, the unconstrained maximization of efficacy created white points that were not of acceptable quality. This can be confirmed by looking at the mean Δuv results in Figure 4. However, in addition to adding nonlinear constraints about Δuv, the setpoints of the LEDs could be bounded. In other words, when maximizing efficacy, three wavelengths could represent the minimum solution rather than two (e.g., a whitepoint consists of cyan, amber, and red). This would improve the quality of the whitepoint.

Finally, a three-channel RGB color sensor was calibrated using samples of daylight as well as 31 whitepoints from this test source using Equation (6). The results of using these techniques are given in Figure 5. The graphs imply that when the TCS3414 is calibrated and measuring a similar source, the results are adequate for automated color control in a room. Yet, when the opposite scenario is considered (i.e., we seek the CCT of sunlight using a TCS3414 calibrated using a LED luminaire) the transfer function does not contain enough information to calculate the tristimulus values of this broad-spectrum source. This dependency occurs because of two reasons. The first explanation is that the sensor is limited to three channels (red, green, and blue). This can be remedied by adding additional channels (e.g., increasing the dimensional basis) in which the peak responsivity of each new channel complements the existing red, green, and blue channels. Equation (6) can be readily adapted to account for these additional channels. Our second explanation deals primarily with the responsivity of the sensor itself. Short of using a spectrometer, if the responsivity of the red, green, and blue filters matched those of the standard observer (i.e., a colorimeter), then this dependency would cease to exist. The benefit of using a color sensor, rather than a spectrometer or colorimeter to perform this function, is cost.

5.2 Control of the Lighting Network

Using the results in Sec. 5.1, the network was tested with two pentachromatic sources. The user could select the color and intensity using the sensor node and set the desired illumination by pressing a button. When this button was pressed, the sensor node measured the lighting conditions incident on the sensor and the control computer solved the linear program to optimally adjust lighting intensities according to Equation (11). The chromaticity of the sources were set according to a look up table of optimal points determined by Equation (7). The local

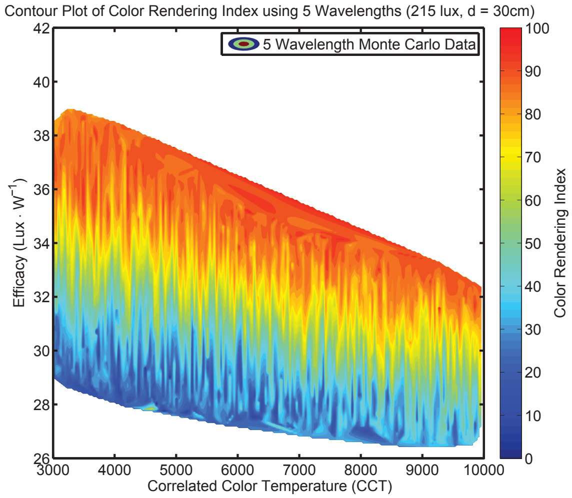

(a)

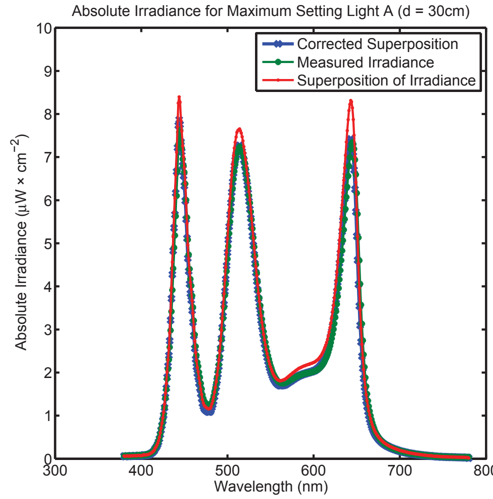

(b)

Figure 3: In (a), the results of the Monte Carlo simulation using five wavelengths at a distance of 30 cm from the source. In (b), the whitepoint (all LEDs at maximum), superposition of the individual spectra, and temperature corrected spectra are plotted. The corrected superposition is in accordance with the measured whitepoint.

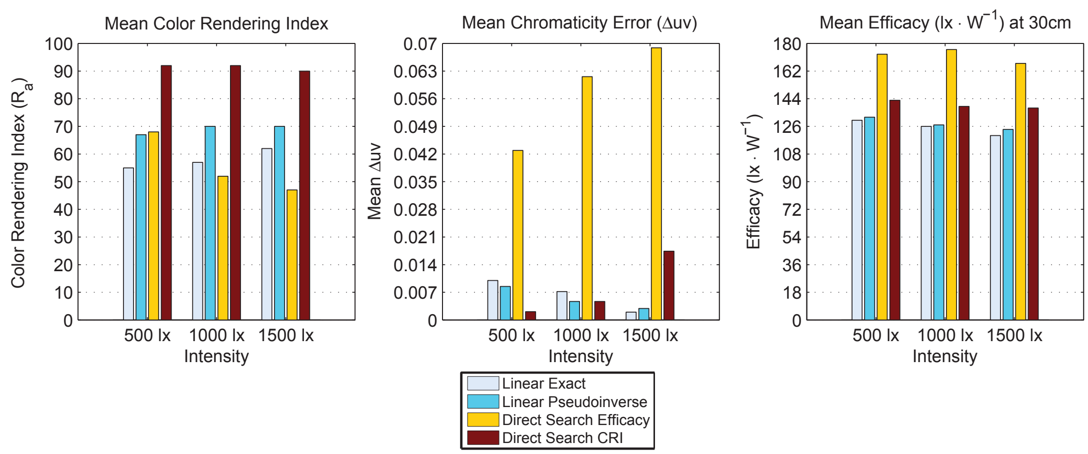

Figure 4: Results obtained from study of linear and nonlinear methods of color control with the spectrometer head positioned 30 cm from the test source. To generate these data, the average of the graphed parameter was taken for the eleven tested white points. Here, we see the effectiveness of the direct search algorithm. It is capable of outperforming the exact and overdetermined methods of control with respect to CRI. In the case where efficacy is maximized, this technique creates white points 28% more efficiently at the cost of increased Δuv error. Alternatively, rather than make minimizing Δuv error in the objective function, Δuv could be specified as a nonlinear inequality constraint at the cost of completion time. We also note the marginal improvement of the overdetermined method over the exact method. The average time of completion for each white point was approximately 15-30 seconds on an Intel Core 2 Quad, making this a feasible method for factory calibration.

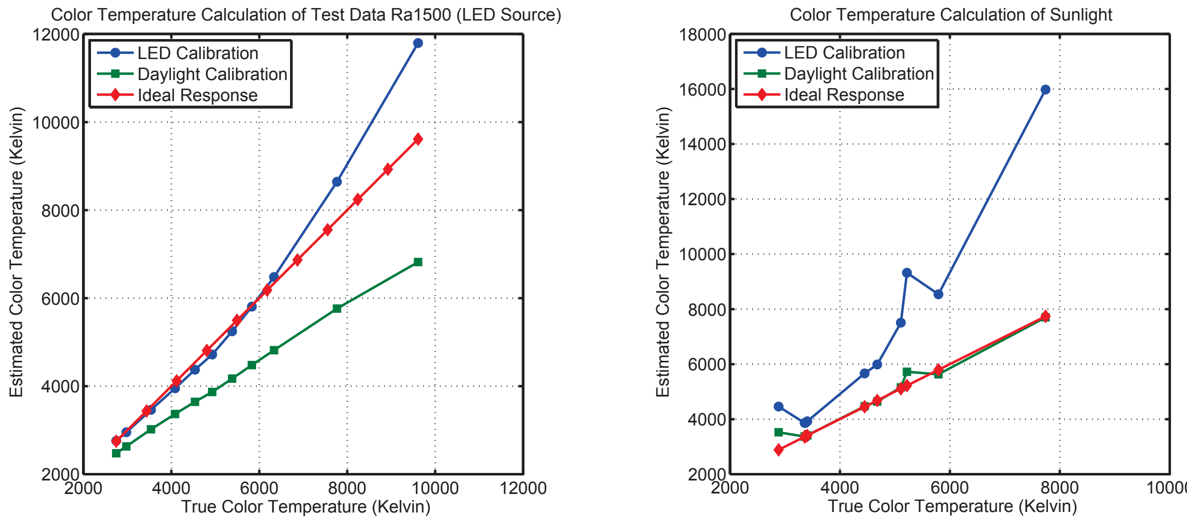

(a) (b)

Figure 5: Comparison of calibration results. In (a) the color sensor is calibrated using either an LED source or daylight and its response to LED irradiance is given. In (b), the color sensor is calibrated the same way, but its response to daylight irradiance is given. The results correlate well with the calibration method employed. However, in (a) the linearity of the daylight calibration method may make it applicable in measuring a broad range of sources.

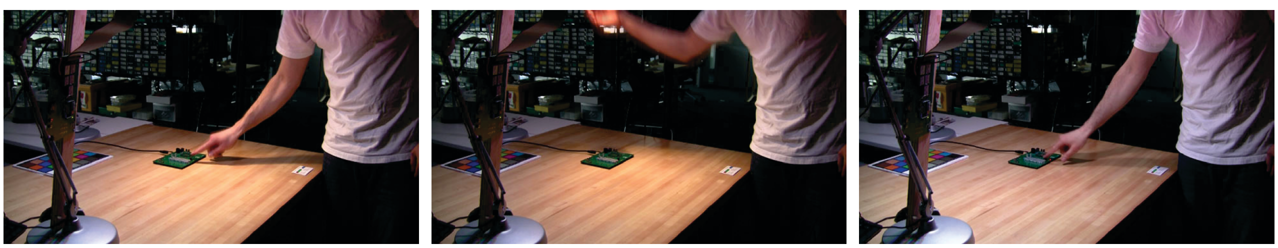

Figure 6: An example of the system optimizing the lighting across two fixtures to achieve a desired illuminance at the sensor node. First, an uncalibrated workspace with additional ambient light (left). The workspace after setting the intensity and calibrating (middle). The workspace after turning off the ambient source and calibrating (right). Energy is minimized once the system is calibrated. When the ambient light source is removed, we expect that the intensity of the system will be increased (right). Although the beam angle of the prototypes is quite large, the system adjusted the illumination to achieve the lighting goal at the sensor location, not across the surface.

problem (the minimization of energy while meeting the illuminance requirements) is solved each time the user presses the button. This scenario is visually depicted in Figure 6.

For long-term testing, we created an interactive lighting testbed using commercially available adjustable white luminaires (Figure 7). Using the sensor node and Equation (11), the system continuously monitors and solves the linear program based on the data taken after the button is pressed. Measuring the controlled and uncontrolled sources in the space is required each time the node is moved. Dark measurements are logged every 10 minutes, which allows us to track the ambient illuminance during testing. The users can adjust their illuminance and color preferences at any time, thus changing the linear constraints of the program. Additionally, the different forward voltages and number of LEDs per channel in the white luminaires makes certain color temperatures more energy efficient at the expense of the color rendering index.

Early results of illuminance tracking and energy savings are given in Figure 8 for two users of the network. In

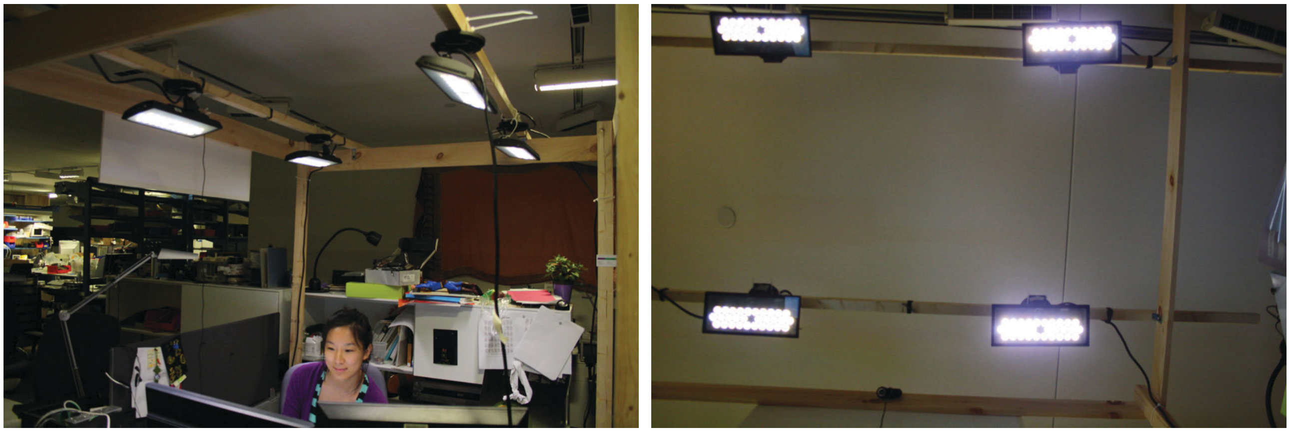

Figure 7: The testbed (left) constructed to study the effects of using a linear program to optimize the lighting conditions based upon the user's preferences of illuminance, color, and ambient light. Looking up towards the lights from the work surface (right).

Figure 8a, we observe that the user adjusted the illuminance at three points during the experiment and that for the first three hours, the measured illuminance of the ambient was greater than the preference, thus the lights remained off. In Figure 8b, the user prefers a higher illuminance and actively adjusts the illuminance controls (17:30). The average ambient lux in both test scenarios is similar except that with subject #2, we observe an increased power consumption at 18:30, corresponding to the user incorrectly placing the sensor node and not pressing the button (evidence of this behavior is given in Figure 9). The present drawback of the system is that user's must manually recalibrate the system when the sensor board is repositioned, otherwise the program continues to optimize for conditions are that are non-existent.

The results indicate that accounting for ambient light and dynamic illuminance preferences yields favorable reductions in lighting network energy usage. However, given the present linear constraint, it is possible that lights whose contribution is not required will be turned off. Ongoing studies are required to examine whether this is distracting and unwanted by the user. One alternative method is requiring the network to be of constant illuminance. In this case, the control system is simply required to track the measured illuminance and user-set illuminance and minimize the error between the two.

6. FUTURE WORK

By creating white light in which the wavelengths are centered closer to 555 nm (the peak of our photopic efficiency), we can create near-similar white points in which we maximize efficacy rather than the color rendering index. But, it is important to point out that the present efficacy of phosphor-pumped LEDs exceeds those of any active-emitter system. Yet, the same tradeoffs present in active-emitter design are encountered in tunable white phosphor systems (e.g., the efficacy and CRI of warm and cool phosphors). Therefore, the greater challenge in any design employing spectral optimization is encouraging the user to sacrifice one parameter for another. It is also important to understand that the results of the numerical techniques presented here are applicable to a wider range of problems. For example, we could choose to optimize a single color rendering parameter, such as R_8, or modify the evaluation function to maximize certain attributes of the Color Quality Scale (CQS).[34,35] Our results on the use of a tri-color sensor to calculate the correlated color temperature of a space require the device to measure the irradiance of a limited set of sources. Using a sensor with more than three channels may be one particular way to lessen the error. A short-term goal includes improving our low-cost method of calculating correlated color temperature by adding additional sensing channels to improve accuracy.

The lighting network calibration is needed to optimize the energy consumption of the network. At present, this requires the user to manually press a button. The drawback is that when the node is moved or relocated, the system will continue to adjust the lighting according to the previous lighting measurement. Thus, future

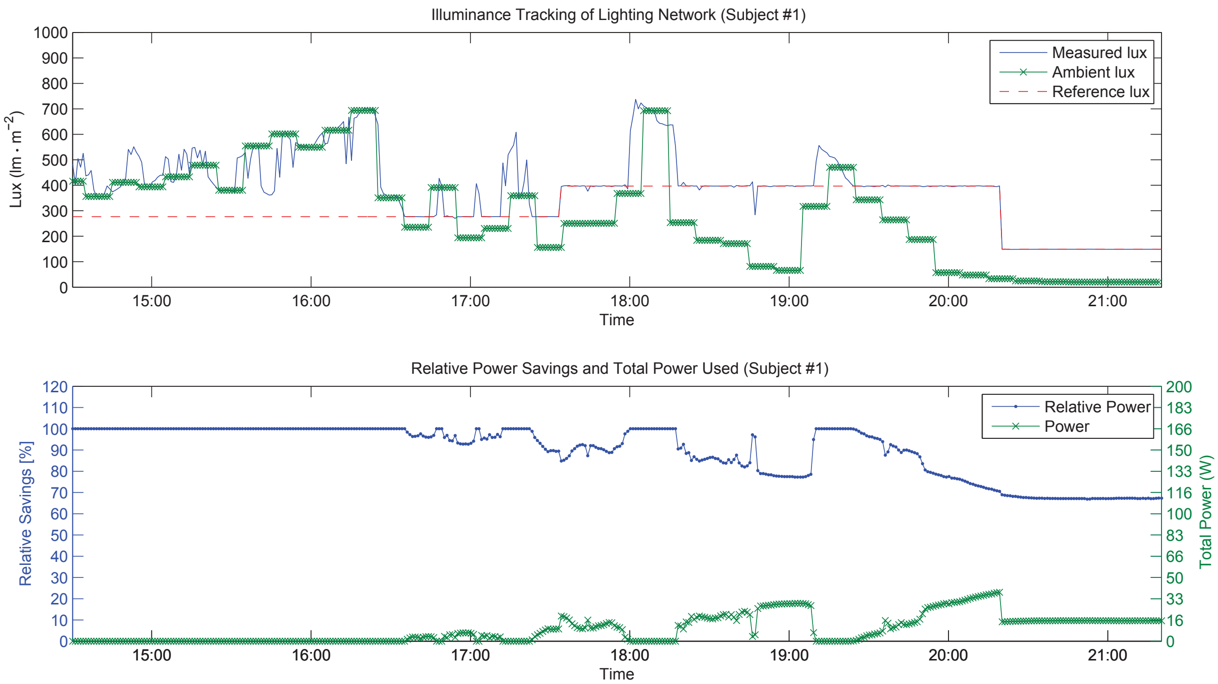

(a)

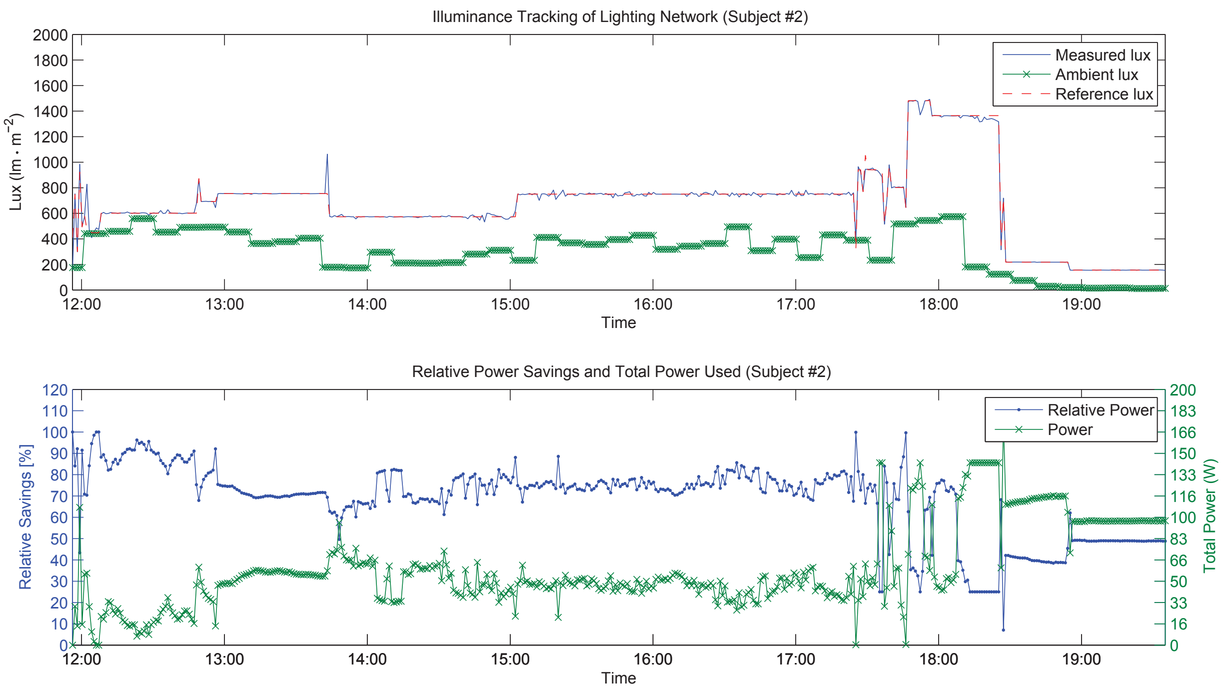

(b)

Figure 8: Test results for two subjects using the phosphor-based lighting network. The relative power savings are based upon the lighting network set to maximum intensity (analogous to fluorescent lighting in an office). The reference lux is set by adjusting the illuminance slider on the sensor board. In (b), at approximately 17:30, subject #2 made several rapid changes to the reference illuminance and we see that the system tracks these changes well. In this figure, ambient light was logged every ten minutes and the sensor data was logged every minute. In these experiments, the closed-loop control ran at approximately 10 Hz.

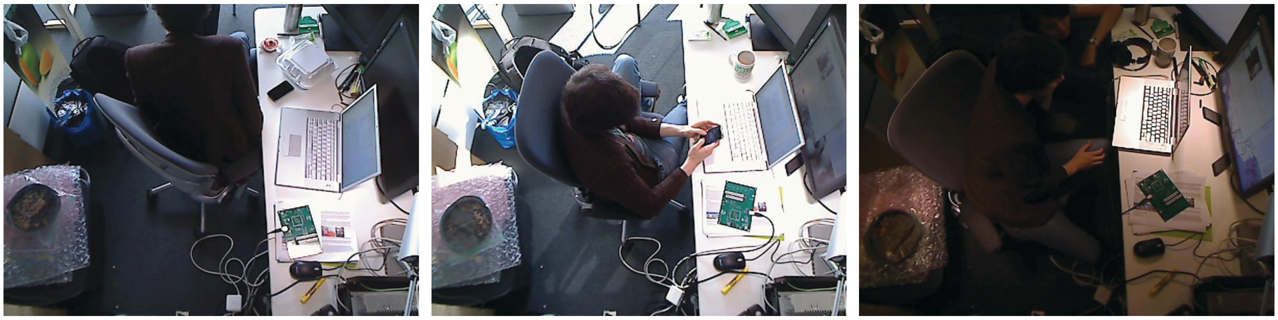

Figure 9: Images (logged automatically every minute) of subject #2 during the experiment depicting the lighting environment at 15:00 (left), 18:00 (middle), and 19:00 (right). At approximately 18:30 (cross-referenced with Figure 8b), the total power consumption versus the desired illuminance is in a unique state. In the final frame (right) we see that the light is focused on the computer and not at the sensor node. Thus, the measured illuminance is not the illuminance at the area of interest, and the power consumption and reference setpoint are not in agreement.

versions of the sensor node will focus on automatic measurements of the incident light using an accelerometer or motion sensor to detect activity. Another possibility is accounting for multiple points of measurement, such that the user could specify a specific area of illumination. We also plan to increase the speed at which the network can adapt to changing conditions by implementing the control functions on a real-time operating system.

Since the light sources are dimmed using PWM, measuring the lighting conditions requires either setting the LEDs to a maximum setting (e.g., the optical sensors no longer detect switching), or the use of a min/max type operation on the sensor node (currently implemented). The challenge with using min/max is that multiple PWM sources operating at different fundamental frequencies produce aliasing in the illuminance sensors that are not low-pass filtered. Thus, during this measurement, the light fixtures in the network are switched on and off in a way such that the ambient light and the contribution of each source are measured. This can lead to noticeable visual effects.

We plan to study alternative methods of calibrating the network that minimize unwanted artifacts of calibration. For instance, the duty cycle of the sources could be used to synchronize the reading and polling of the optical sensors on the sensor board. We could also set the fundamental PWM frequencies in a lighting network such that a sensor node with multiple bandpass filters could recover the unique illuminance of each source. Another approach requires the use of high-irradiance near-infrared LEDs, in which a predetermined transfer function relates the measured IR to intensity or illuminance. At the fixture, the IR source is modulated according to the present system setpoint (an internal model calculates the total candelas, not radiant intensity).

Future implementations will also control incandescent lights, dimmable fluorescent sources, and the amount of daylight in a space (via motorized blinds). Integrating cameras into the network will enable us to visualize the light fields present on the surface to enable measuring and controlling entire areas. It also offers the possibility of performing network localization. Additionally, it will expand our measurement capabilities and enable new forms of human control of the lighting network as we plan on using the vision system to incorporate inferred user activities and free gesture in the lighting control.

7. CONCLUSION

In this paper, the photometric and optical challenges associated with energy efficient lighting and LEDs are solved using numerical optimization. We report the improved photometric properties of a pentachromatic light source using these techniques. We also present a prototype sensor node which measures illuminance and color temperature and that allows the user to specify the desired illuminance and color at the operating surface. Additionally, we demonstrate a phosphor-based system controlled by this sensor node, in which the user-specified operating point is optimized to reduce the current using a linear program.

ACKNOWLEDGMENTS

We wish to thank John Warwick and the team at Philips-Color Kinetics for the donation of the color-adjustable white fixtures for the control testbed. We also want to thank the Responsive Environments Group at the MIT Media Laboratory for their insight and help during testing. This research is directly funded by the MIT Media Laboratory.

REFERENCES

[1] U.S. Energy Information Administration., [*Energy Consumption by Sector*], Annual Energy Review, 2006 (2007).

[2] Navigent Consulting, Inc., "Solid-state lighting research and development portfolio: Multi-year program plan fy'09-fy'15," tech. rep., Lighting Research and Development Building Technologies Program, Office of Energy Efficiency and Renewable Energy, U.S. Dept. of Energy, Chicago (2009).

[3] Singhvi, V., Krause, A., Guestrin, C., Garrett, Jr, J. H., and Matthews, H. S., "Intelligent light control using sensor networks," in [*SenSys '05: Proceedings of the 3rd international conference on Embedded networked sensor systems*], *SenSys'05*, 218–229, ACM (2005).

[4] Wen, Y. J., Granderson, J., and Agogino, A. M., "Towards embedded wireless-networked intelligent daylighting systems for commercial buildings," in [*Proceedings of the IEEE International Conference on Sensor Networks, Ubiquitous, and Trustworthy Computing*], *Proc. IEEE* **1**, 326–331, IEEE Computer Society (2006).

[5] Aldrich, M., *Dynamic Solid State Lighting*, Master's thesis, Massachusetts Institute of Technology (2010).

[6] Zhao, N., *Smart Solid-State Lighting Control*, Master's thesis, RWTH Aachen University (2010).

[7] Crisp, V. H. C., "Preliminary study of automatic daylight control of artificial lighting," *Lighting Research and Technology* **9**(1), 31–41 (1977).

[8] Hunt, D. R. G., "Simple expressions for predicting energy savings from photo-electric control of lighting," *Lighting Research and Technology* **9**(2), 93–102 (1977).

[9] Crisp, V. H. C., "The light switch in buildings," *Lighting Research and Technology* **10**(2), 69–82 (1978).

[10] Hunt, D. R. G., "Improved daylight data for predicting energy savings from photoelectric controls," *Lighting Research and Technology* **11**(1), 9–23 (1979).

[11] Crisp, V. H. C. and Henderson, G., "The energy management of artificial lighting use," *Lighting Research and Technology* **14**(4), 193–206 (1982).

[12] Park, H., Burke, J., and Srivastava, M. B., "Design and implementation of a wireless sensor network for intelligent light control," in [*Proceedings of the 6th international conference on Information processing in sensor networks*], *IPSN'07*, 370–379, ACM (2007).

[13] Machado, C. and Mendes, J. A., "Automatic light control in domotics using artificial neural networks," in [*World Academy of Science, Engineering and Technology*], **44**, 813– (August, 2008).

[14] Mozer, M., "The neural network house: An environment that adapts to its inhabitants," in [*Proc. AAAI Spring Symp. Intelligent Environments*], (1998).

[15] Muthu, S., Schuurmans, F. J., and Pashley, M. D., "Red, green, and blue LED based white light generation: issues and control," in [*Industry Applications Conference, 2002. 37th IAS Annual Meeting. Conference Record of the*], *Proc. IEEE* **4**, 327–333 (2002).

[16] Ashdown, I. E., "Neural networks for LED color control," *Proc. SPIE* **5187**(1), 215–226 (2004).

[17] Ackermann, B., Schulz, V., Martiny, C., Hilgers, A., and Zhu, X., "Control of LEDs," in [*Industry Applications Conference, 2006. 41st IAS Annual Meeting. Conference Record of the*], *Proc. IEEE* **5**, 2608–2615, IEEE (2006).

[18] Schubert, E. F., Kim, J. K., Luo, H., and Xi, J.-Q., "Solid-state lighting - a benevolent technology," *Reports on Progress in Physics* **69**(12), 3069–3099 (2006).

[19] Narendran, N., Deng, L., Pysar, R. M., Gu, Y., and Yu, H., "Performance characteristics of high-power light-emitting diodes," *Proc. SPIE*(1), 267–275 (2004).

[20] Zukauskas, A., Vaicekauskas, R., Ivanauskas, F., Gaska, R., and Shur, M. S., "Optimization of white polychromatic semiconductor lamps," *Appl.Phys.Lett.* **80**(2), 234–236 (2002).

[21] Schubert, E. F. and Kim, J. K., "Solid-state light sources getting smart," *Science* **308**(5726), 1274–1278 (2005).

[22] Stanikunas, R., Vaitkevicius, H., Svegzda, A., Viliunas, V., Bliznikas, Z., Breive, K., Vaicekauskas, R., Novickovas, A., Kurilcik, G., Zukauskas, A., Gaska, R., and Shur, M. S., "Polychromatic solid-state lamps versus tungsten radiator: hue changes of munsell samples," *J.Phys.D* **38**(17), 3202–3207 (2005).

[23] Lei, Z., Xia, G., Ting, L., Xiaoling, G., Qiao Ming, L., and Guangdi, S., "Color rendering and luminous efficacy of trichromatic and tetrachromatic LED-based white LEDs," *Microelectron.J.* **38**(1), 1–6 (2007).

[24] Zukauskas, A., Vaicekauskas, R., Ivanauskas, F., VaitkeviCius, H., and Shur, M. S., "Rendering a color palette by light-emitting diodes," *Appl.Phys.Lett.* **93**(2), 021109– (2008).

[25] Robertson, A. R., "Computation of correlated color temperature and distribution temperature," *J.Opt.Soc.Am.* **58**(11), 1528–1535 (1968).

[26] Audet, C. and Dennis, Jr, J., "Mesh adaptive direct search algorithms for constrained optimization," *SIAM J.on Optimization* **17**(1), 188–217 (2006).

[27] Torczon, V., "On the convergence of pattern search algorithms," *SIAM J.on Optimization* **7**(1), 1–25 (1997).

[28] The MathWorks, Inc., *Global Optimization Toolbox 3*. The Mathworks, Inc., 3 Apple Hill Drive Natick, MA 01760-2098, 14 ed. (March 2010).

[29] Jones, D. R., Perttunen, C. D., and Stuckman, B. E., "Lipschitzian optimization without the lipschitz constant," *J.Optimiz.Theory Appl.* **79**(1), 157–181 (1993).

[30] Hooke, R. and Jeeves, T. A., "'Direct search' solution of numerical and statistical problems," *J.ACM* **8**(2), 212–229 (1961).

[31] Rosenbrock, H. H., "An automatic method for finding the greatest or least value of a function," *The Computer Journal* **3**(3), 175–184 (1960).

[32] Nelder, J. A. and Mead, R., "A simplex method for function minimization," *The Computer Journal* **7**(4), 308–313 (1965).

[33] Wyszecki, G. and Stiles, W. S., [*Color Science : Concepts and Methods, Quantitative Data and Formulae*], vol. 2, Wiley, New York (1982).

[34] Davis, W. and Ohno, Y., "Toward an improved color rendering metric," *Proc. SPIE* **5941**(1) (2005).

[35] Ohno, Y., "Spectral design considerations for white LED color rendering," *Opt.Eng.* **44**(11), 111302– (2005).